

Sterile Neutrinos in astrophysical and cosmological sauce^{*)}

Marco Cirelli¹⁾

1. Physics Dept. - Yale University, New Haven, CT 06520, USA

Abstract — The study of sterile neutrinos has recently acquired a different flavor: being now excluded as the dominant solution for the solar or atmospheric conversions, sterile neutrinos, still attractive for many other reasons, have thus become even more elusive. The present relevant questions are: which subdominant role can they have? Where (and how) can they show up? Cosmology and supernovæ turn out to be powerful tools to address these issues. With the most general mixing scenarios in mind, I present the analysis of many possible effects on BBN, CMB, LSS, and in SN physics due to sterile neutrinos. I discuss the computational techniques, present the state-of-the-art bounds, identify the still allowed regions and study some of the most promising future probes. I show how the region of the LSND sterile neutrino is excluded by the constraints of standard cosmology.

1 Introduction

The study of sterile neutrinos (namely: additional light fermionic particles that are neutral under all Standard Model gauge forces, but can be a non-negligible ingredient of our world through their mixing with e, μ, τ neutrinos) has recently acquired a different flavor: the established solar and atmospheric anomalies seem produced by oscillations among the three active neutrinos [2, 3] so that their explanation in terms of oscillation into a ν_s state (which was viable and fairly popular up to a few years ago) is believed to be now ruled out as the dominant mechanism. This means that the **relevant questions concerning sterile neutrinos nowadays** have become: •which is the *subdominant* role still possible for sterile neutrinos in solar and atmospheric neutrinos? •where can we detect the effects of a sterile neutrino? i.e. which are the most sensitive experiments (in astrophysics, cosmology or man-made set-ups) in which sterile neutrinos can be discovered? •how can we detect the effects of a sterile neutrino? i.e. which are the signatures of its presence?

To answer these questions, the investigation on sterile neutrinos requires a more extensive and deep approach. Indeed, for instance, most of the previous analysis used to consider only the peculiar oscillation pattern that gives the simplest physics: the initial active neutrino $|\nu_a\rangle$ (ν_e in the case of solar neutrinos, ν_μ in the case of the atmospheric ones) oscillates into an energy-independent mixed neutrino $\cos\theta_s|\nu'_a\rangle + \sin\theta_s|\nu_s\rangle$. This of course leaves unexplored the largest part of the parameter space. Sometimes, moreover, previous analysis used to neglect for simplicity the mixing among active neutrinos (this is the case of most studies on the sterile effects in cosmology or in supernovæ). Such a mixing is now established and its parameters are reasonably pinned down.

These considerations motivate the analysis performed in [1] and presented here, which considers and includes:

- a. any possible $\nu_{e,\mu,\tau} - \nu_s$ mixing pattern;
- b. the established $\nu_e - \nu_{\mu,\tau}, \nu_\mu - \nu_\tau$ mixings;
- c. all possible neutrino sources and contexts (cosmology (BigBang Nucleosynthesis-BBN, Cosmic Microwave Background-CMB, Large Scale Structures-LSS), astrophysics (the Sun, supernovæ-SNe...), atmospheric neutrinos, reactor and accelerator experiments...),

^{*)}Based on the Proceedings for the 10th International Symposium on Particles, Strings and Cosmology (PASCOS '04), 16-22 August 2004, Northeastern University, Boston, MA, USA and for the XVI Incontri sulla Fisica delle Alte Energie (IFAE), 14-16 April 2004, Torino, Italy.

The purpose is to set the state-of-the-art bounds on the active-sterile mixing parameters (in each context separately and then in a combined way) and to identify the most promising future probes. Since the different cosmological quantities and the observables of SN physics turn out to be very important to this aim, investigating complementary regions and allowing the application of techniques that extend to other fields, these are the contexts on which I focus in these Proceedings.

Before going to the details, let's stress that now that the hunger of sterile neutrinos for the solar and atmospheric anomalies is over, nevertheless **sterile neutrinos are even more attractive** for at least two sets of reasons.

First, from a top-down point of view, sterile fermions that are naturally light or cleverly lightened arise in many theories that try to figure out what is beyond the Standard Model. To begin, slightly beyond the context of the SM, the right handed neutrino is an obvious candidate, to complete the lepton sector in similarity (symmetry?) with the quark one. In this case, actually, three states (one per family) would be natural. More broadly, several (SuSy-/GUT-/string-/ED- inspired) SM gauge singlets line up awaiting for consideration (axino, branino, dilatino, familino, Goldstino, Majorino, mirror fermion, modulino, radino...) [4]. The origin and the load of information of any of these particles can be very different, but from an effective point of view we simply need to parameterize their mixing with the active neutrinos in terms of mixing angles and Δm^2 (see below) to include them all in the analysis. Independently from the specific model, the discovery of a new light particle would be of fundamental importance and deserves to be investigated per se.

Second, from a more phenomenological bottom-up perspective, sterile neutrinos are repeatedly pointed as a possible explanation for several puzzling situations in particle physics, astronomy and cosmology. For instance, they have been invoked [5] to account for the origin of the pulsar kicks, to constitute a Dark Matter candidate, to explain (via their decay) the diffuse ionization of the Milky Way, to help the r-process nucleosynthesis in the environment of exploding stars, to interpret the slightly too low Argon production in the Homestake experiment... and notoriously to explain the LSND claimed evidence of oscillations [6]. Any one of these puzzles, in general, points to specific sterile neutrinos (i.e. with a specific mixing pattern with the active ones) and it is therefore worthwhile to explore them in an extensive way.

2 Four neutrino mix

In absence of sterile neutrinos, we denote by U the usual 3×3 mixing matrix that relates neutrino flavor eigenstates $\nu_{e,\mu,\tau}$ to active neutrino mass eigenstates $\nu_{1,2,3}$ as $\nu_\ell = U_{\ell i} \nu_i$. The extra sterile neutrino can then mix with a **mixing angle** θ_s with an **arbitrary combination of active neutrinos**, which we identify by a complex unit 3-vector \vec{n} ¹⁾

$$\vec{n} \cdot \vec{\nu} = n_e \nu_e + n_\mu \nu_\mu + n_\tau \nu_\tau = n_1 \nu_1 + n_2 \nu_2 + n_3 \nu_3 \quad (n_i = U_{\ell i} n_\ell). \quad (2)$$

So, in particular, the 4th mass eigenstate is given by $\nu_4 = \nu_s \cos \theta_s + n_\ell \nu_\ell \sin \theta_s$. We allow all possible values of its **mass** m_4 ('the mass of the sterile neutrino', in the small mixing case).

Such a formalism is completely general and covers of course all the possible mixing patterns. We need to choose, however, some intuitive limiting cases to present the results in the following:

- **Mixing with a flavor eigenstate** (fig. 1a): the sterile neutrino oscillates into one of the active flavors ($\vec{n} \cdot \vec{\nu} = \nu_\ell$ with $\ell = e$ or μ or τ). Therefore there are 3 different active-sterile Δm^2 (which cannot all be smaller than the observed splittings $\Delta m_{\text{sun,atm}}^2$, see figure).
- **Mixing with a mass eigenstate** (fig. 1b): the sterile neutrino oscillates into a matter eigenstate, that consists therefore of mixed flavor ($\vec{n} \cdot \vec{\nu} = \nu_i$, with $i = 1$ or 2 or 3). There is one single Δm^2 , which can be arbitrarily small.

¹⁾In this way \vec{n} and θ_s , together with the four neutrino masses, simply reorganize in a more intuitive way all the parameters of the most generic 4×4 Majorana neutrino mass matrix, which contains 4 masses, 6 mixing angles and 6 CP-violating phases, of which 3 affect oscillations. The 4×4 neutrino mixing matrix V that relates flavor to mass eigenstates as $\nu_{e,\mu,\tau,s} = V \cdot \nu_{1,2,3,4}$ is expressed in this parameterization by

$$V = \begin{pmatrix} 1 - (1 - \cos \theta_s) \vec{n}^* \otimes \vec{n} & \sin \theta_s \vec{n}^* \\ -\sin \theta_s \vec{n} & \cos \theta_s \end{pmatrix} \times \begin{pmatrix} U & 0 \\ 0 & 1 \end{pmatrix} \quad (1)$$

Commonly, V is instead parameterized as $V = R_{34} R_{24} R_{14} \cdot U_{23} U_{13} U_{12}$ when studying sterile mixing with a flavor eigenstate. Here R_{ij} represents a rotation in the ij plane by angle θ_{ij} and U_{ij} a complex rotation in the ij plane. θ_{14} or U_{e4} give rise to ν_e/ν_s mixing, θ_{24} or $U_{\mu 4}$ to ν_μ/ν_s mixing, and θ_{34} or $U_{\tau 4}$ to ν_τ/ν_s mixing. When studying the mixing with a mass eigenstate, the parameterization of V is changed to $V = U_{23} U_{13} U_{12} \cdot R_{34} R_{24} R_{14}$. Now θ_{i4} gives rise to ν_i/ν_s mixing and so on. Our parameterization is more convenient because \vec{n} already encrypts in a natural way the information on which active states mix with the ν_s , while θ_s simply expresses the size of the mixing.

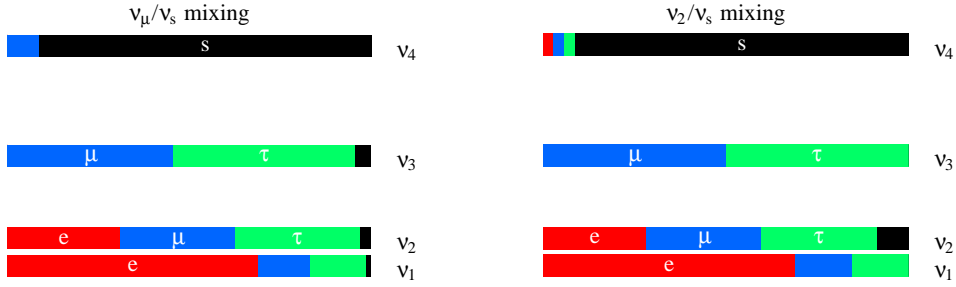


Figure 1: Basic kinds of four neutrino mass spectra. *Left: sterile mixing with a flavor eigenstate (ν_μ in the picture).* *Right: sterile mixing with a mass eigenstate (ν_2 in the picture).*

In the case of mixing with a matter eigenstate, we will consider also the situation in which the (mostly) sterile state is lighter than the (mostly) active state with which it mixes (imagine the ν_4 state lowered below ν_2 in figure 1b): it is represented by the portion of $\theta_s > \pi/4$ in our plots.

We assume that active neutrinos have normal hierarchy, $\Delta m_{23}^2 > 0$. Finally, we assume $\theta_{13} = 0$. We verified that using $\theta_{13} \sim 0.2$, the maximal value allowed by present experiments, leads to minor (in some cases) or no (in other cases) modifications, that we do not discuss.

3 Sterile Neutrinos in cosmological sauce

Generalities: The Early Universe can be a powerful laboratory for neutrino physics, and therefore in particular for the physics of sterile neutrinos. The fundamental reasons for this basic fact are simply listed:

- (light) neutrinos are very abundant (namely “as abundant as photons”) for a long period of the evolution of the Universe, keeping thermal equilibrium until $T \sim \text{few MeV}$;
- in a Friedman-Robertson-Walker standard cosmology, the total energy density is a crucial parameter that sets the expansion rate of the Universe; since that energy is predominantly stored in the relativistic species, namely electrons, positrons, photons and all species of neutrinos, for $T \simeq 100 \text{ MeV} \rightarrow 1 \text{ MeV}$, it is evident that the relative abundance of neutrinos (e.g. increased by the presence of additional states) is a very relevant quantity;
- the early plasma is so dense that neutrinos are initially trapped and undergo peculiar matter effects while the density decreases as a consequence of the expansion;
- the detailed balance of the different species of neutrinos among themselves can also be important for processes that distinguish flavor: for instance, the ν_e density affects the $n \rightarrow p$ conversion and therefore is imprinted in the primordial ratio of n/p that we read today (see below).

We have access to several different windows during the history of the Universe. From them we get a sensitivity to neutrino properties (masses, oscillation parameters...) that is nowadays competitive with direct measurements and even offers a brighter prospective of improvements in the near future, making the study of quantitative neutrino cosmology worthwhile.

BBN: BigBang Nucleosynthesis occurs at $T \sim (1 \div 0.1) \text{ MeV}$ and describes the era when the light elements were synthesized [7]. Given a few input parameters (the effective number N_ν of thermalized relativistic species, the baryon asymmetry $n_B/n_\gamma = \eta$, and possibly the $\nu_\ell/\bar{\nu}_\ell$ lepton asymmetries) BBN successfully predicts the abundances of several light nuclei. Today η is best determined within minimal cosmology by CMB data to be $\eta = (6.15 \pm 0.25)10^{-10}$ [8]. Thus, neglecting the lepton asymmetries (see below), basically one uses the observations of primordial abundances to test if $N_\nu = 3$ as predicted by the SM²⁾. This is what is often done [10], using state-of-the-art, publicly available codes [11]. We need however to do something slightly more refined: indeed, N_ν is an effective parameter that sums up and does not distinguish the relative contributions of the various neutrinos

²⁾For the sake of precision, relaxing the hypothesis of instantaneous neutrino freeze-out and carefully including the partial neutrino reheating from e^+e^- annihilations, the related spectral distortions and finite temperature QED small effects, the SM prediction is actually $N_\nu \simeq 3.04$ [9]. The deviations due to any exotic phenomenon (including sterile neutrinos) go on top of this.

(3 active and 1 (or more) sterile), which can instead be different according to the mixing patterns; moreover, in general, the neutrino populations can have a peculiar behavior in time (temperature) which would be concealed by the use of N_ν .

For these reasons, in our computation we use as variables the four neutrino densities ³⁾ $\rho_{\nu_e}, \rho_{\nu_\mu}, \rho_{\nu_\tau}, \rho_{\nu_s}$: we follow their evolution with the temperature during the whole period of BBN, for each possible choice of the sterile mixing parameters. Starting (conservatively) from a zero initial abundance of the sterile neutrino, at a certain point oscillations start producing it [12]. This essentially happens when the plasma effects/thermal masses for the (active) neutrinos cease to be dominant compared to the vacuum masses, as the Universe expands and cools; at what point precisely (and how efficiently) the production occurs is something which is determined by the sterile mixing parameters. In the meanwhile, other cosmological processes occur, as standard: at $T \sim \text{few MeV}$ neutrinos freeze-out (i.e. loose thermal equilibrium with the bath, but they still take part in the $n \leftrightarrow p$ reactions, see below); at $T \sim 1 \text{ MeV}$ e^+e^- annihilate etc...

More precisely, we follow the time evolution of the full 4×4 density matrices ϱ and $\bar{\varrho}$ (written in the flavor basis), of which the four neutrino densities above constitute the diagonal. In absence of neutrino asymmetries, the neutrino and antineutrino sectors decouple and proceed identically, so we focus on the neutrinos for definiteness. The kinetic equations for such matrices must take into account (i) the vacuum oscillations (active-active and active-sterile), (ii) the matter effects in the primordial plasma, (iii) the $\nu e \leftrightarrow \nu e$ scattering reactions and the $\nu\nu \leftrightarrow ee$ annihilation reactions. They read [12, 13, 14]

$$\frac{d\varrho}{dt} \equiv \frac{dT}{dt} \frac{d\varrho}{dT} = -i[\mathcal{H}_m, \varrho] - \{\Gamma, (\varrho - \varrho^{\text{eq}})\} \quad (3)$$

\mathcal{H}_m is the Hamiltonian in matter, composed by the vacuum Hamiltonian in the flavor basis and the matter potentials V_l for each flavor: these consist of the thermal masses for the neutrinos in the primordial plasma, rapidly decreasing with T . The usual MSW potential is in this case subdominant because the plasma is charge symmetric.

$$\mathcal{H}_m = \frac{1}{2E_\nu} \left[V \text{diag}(m_1^2, m_2^2, m_3^2, m_4^2) V^\dagger + E_\nu \text{diag}(V_e, V_\mu, V_\tau, 0) \right] \quad (4)$$

$$\begin{aligned} V_e &= -\frac{199\sqrt{2}\pi^2}{180} \frac{\zeta(4)}{\zeta(3)} G_F \frac{T_\nu}{M_W^2} \left(T^4 + \frac{1}{2} T_\nu^4 \cos\theta_W \varrho_{ee} \right) \\ V_{\mu,\tau} &= -\frac{199\sqrt{2}\pi^2}{180} \frac{\zeta(4)}{\zeta(3)} G_F \frac{T}{M_W^2} \left(\frac{1}{2} T_\nu^4 \cos\theta_W \varrho_{\mu\mu,\tau\tau} \right) \\ V_s &= 0 \end{aligned} \quad (5)$$

Concerning the reaction part, it can be shown that one has to use: in the equations for the off-diagonal components of ϱ , $\Gamma_{\text{tot}} \approx 3.6 G_F^2 T^5$ for ν_e and $\Gamma_{\text{tot}} \approx 2.5 G_F^2 T^5$ for $\nu_{\mu,\tau}$; in the equations for the diagonal components, $\Gamma_{\text{ann}} \approx 0.5 G_F^2 T^5$ for ν_e and $\Gamma_{\text{ann}} \approx 0.3 G_F^2 T^5$ for $\nu_{\mu,\tau}$. $\varrho^{\text{eq}} = \text{diag}(1, 1, 1, 0)$ is the equilibrium value of the density matrix to which the reactions tend. The neutrino freeze-out occurs when these Γ 's are overwhelmed by the expansion of the Universe.

The determination of $\frac{dT}{dt}$ is in principle quite involved, since we need to keep track of the several phenomena that go on in the range $T \sim 1 \text{ MeV}$ which is under examination. In particular, we want to include the possible extra degrees of freedom (the sterile neutrinos) that are produced by the oscillations and we do not want to neglect the heating due to e^+e^- annihilations. In first approximation, we can use the standard expression $\dot{T} = -H(\rho_{\nu_{\text{tot}}}) T$, where H contains the (temperature dependent) total energy density, including in particular that of all neutrinos.

After solving the neutrino densities evolution with temperature, we can study the relative neutrons/protons abundance, which is the all-important quantity for the outcome of primordial nucleosynthesis, since those are the building blocks of the nuclei that are going to be formed and essentially all neutrons are incorporated into some light element in the process: the neutron abundance at the moment that the synthesis begins practically fixes the proportions of all the products. n/p evolves according to

$$\dot{r} \equiv \frac{dT}{dt} \frac{dr}{dT} = \Gamma_{p \rightarrow n} (1 - r) - r \Gamma_{n \rightarrow p} \quad r = \frac{n_n}{n_n + n_p} \quad (6)$$

$\Gamma_{p \rightarrow n}$ is the total rate for all the $p \rightarrow n$ reactions ($n \rightarrow p e^- \bar{\nu}_e, n \nu_e \rightarrow p e^-, n e^+ \rightarrow p \bar{\nu}_e$) and $\Gamma_{n \rightarrow p}$ for the inverse processes. They depend on the ρ_{ν_e} and $\rho_{\bar{\nu}_e}$ densities computed above. At this point, it is apparent how the production of **sterile neutrinos can enter the game** by

- A. entering in $\rho_{\nu_{\text{tot}}}$ and thus increasing the Hubble parameter H i.e. the expansion rate;
- B. modifying the $\Gamma_{p \rightarrow n}, \Gamma_{n \rightarrow p}$ rates directly, if the $\nu_e, \bar{\nu}_e$ population is depleted by oscillations.

With the value of n/p in hand, finally a network of Boltzmann equations describes how electroweak, strong and electromagnetic processes control the evolution of the various nuclei: $p, n, D, T, {}^3\text{He}, {}^4\text{He}, \dots$

For the purposes of the CMB and LSS bounds discussed below, the neutrino densities at the time of recombination and today are needed. These are simply given by the final outputs (i.e. for $T \ll 0.1 \text{ MeV}$) of the kinetic equations.

We assume a vanishing or negligibly small **neutrino asymmetry** η_ν . Allowing an unnatural large η_ν (namely, much larger than the corresponding asymmetry η in baryons), besides affecting non trivially the evolution [15], means adding an extra relevant parameter, so that one could essentially conceal any sterile effect, at least as long as observations will not be able to break the degeneracy.

³⁾The densities are intended as relative to the photon one, so that $\rho_{\nu_l} \in (0, 1)$.

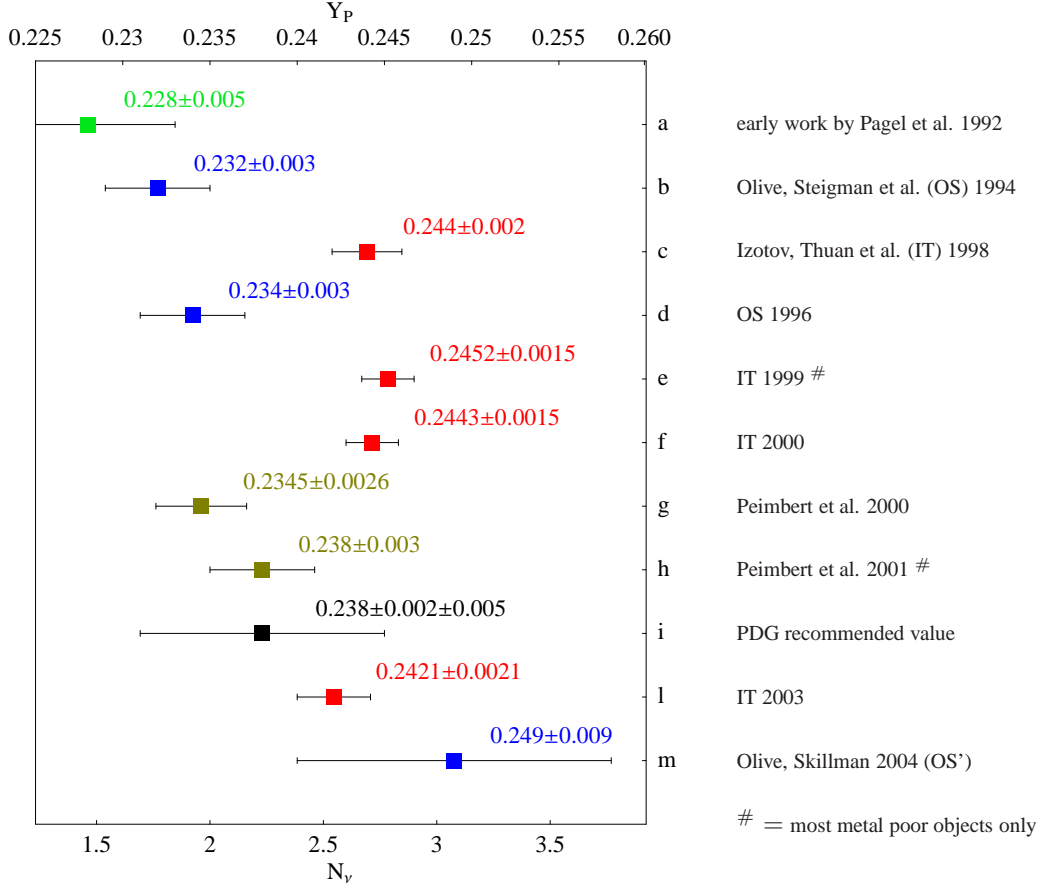


Figure 2: Some recent experimental results in the determination of the primordial ^4He abundance Y_p . The bars correspond to the claimed 1σ errors. The PDG recommended value adds an estimate of the systematic uncertainties (± 0.005). References are in [16].

At the end of the process, we can compute how the light elements abundances are modified and compare them to the observations. We focus on the ^4He abundance, which is today the most sensitive probe of sterile effects, but we also study the Deuterium abundance, which has brighter prospects of future improvements. The observational determinations of both quantities are plagued by controversial systematic uncertainties. For instance, Fig.2 collects some of the most recent results for ^4He [16]. A similar situation, with perhaps less controversy and more overall uncertainty, applies to the case of Deuterium [17]. Conservative estimates are

$$\begin{aligned} Y_p &= 0.24 \pm 0.01, \\ Y_D/Y_H &= (2.8 \pm 0.5) 10^{-5}, \end{aligned} \quad (7)$$

where $Y_X \equiv n_X/n_B$ and Y_p is the traditional notation for $Y_{^4\text{He}}$.

At this point, for ease of presentation, we can even convert the values of the computed primordial abundances back into effective numbers of neutrinos, $N_\nu^{^4\text{He}}$ and N_ν^D . For arbitrary values around the SM value of 3, BBN codes predict [7, 10] the following relations

$$Y_p \simeq 0.248 + 0.0096 \ln \frac{\eta}{6.15 \cdot 10^{-10}} + 0.013(N_\nu^{^4\text{He}} - 3), \quad (8a)$$

$$Y_D/Y_H \simeq (2.75 \pm 0.13) 10^{-5} \frac{1 + 0.11 (N_\nu^D - 3)}{(\eta/6.15 \cdot 10^{-10})^{1.6}}. \quad (8b)$$

The observed abundances of eq.(7) then translate into

$$\begin{aligned} N_\nu^{^4\text{He}} &\simeq 2.4 \pm 0.7, \\ N_\nu^D &\simeq 3 \pm 2. \end{aligned} \quad (9)$$

LSS: Neutrinos can also be studied looking at the distribution of galaxies. The connection lies at the time of the

formation of the anisotropies in the primordial plasma that were the seeds for the formation of the Large Scale Structures (which took place much time later). The point is that the neutrinos, relativistically traveling through the plasma (from which they were decoupled) until their mass was of the order of the temperature, had the effect of smoothing the anisotropies, i.e. they caused a suppression in the power spectrum of the galaxies that is measured today. Qualitatively, light neutrinos traveled relativistically for a long period and therefore delayed the formation of structures characterized by a scale smaller than that of the horizon at the time they became non-relativistic. The more massive the neutrinos are, the earlier they became non-relativistic, the smaller the scale of the horizon was at that time, inside which the perturbations were smoothed, the more suppressed are the large momenta of the LSS power spectrum.

In formulæ, the effect is usually expressed in terms of the quantity Ω_ν , which is related to the sum of the neutrino masses

$$\Omega_\nu h^2 = \frac{\text{Tr}[m \cdot \varrho]}{93.5 \text{ eV}} \quad (10)$$

where m is the 4×4 neutrino mass matrix and ϱ is the 4×4 neutrino density matrix (at late cosmological times), discussed and computed above. In a standard case, the numerator corresponds to $\sum m_{\nu_i}$. In general, the determination of Ω_ν depends on priors and on normalisations, possibly fixed by the CMB spectrum. As a rule of thumb, the present bound [18] and the future expected sensitivity [19] can be summed in

$$\text{present : } \quad \Omega_\nu h^2 \lesssim 10^{-2} \quad (11)$$

$$\text{future : } \quad \Omega_\nu h^2 \lesssim 10^{-3}. \quad (12)$$

CMB: Finally, neutrinos can be studied through the pattern of the CMB anisotropies measured by WMAP (and other experiments). They affect the CMB anisotropies in various ways [20]; the all important quantity is their contribution to the relativistic energy density

$$\text{Tr}[\varrho] = \rho_{\nu_{\text{tot}}} \subset \rho_{\text{rel}} \quad (13)$$

(where again ϱ is the 4×4 neutrino density matrix (at late cosmological times), discussed and computed above), straightforwardly parameterized in terms of an effective number⁴⁾ of neutrinos N_ν^{CMB}

$$\rho_{\text{rel}} = \rho_\gamma \left[1 + \frac{7}{8} \left(\frac{4}{11} \right)^{4/3} N_\nu^{\text{CMB}} \right]. \quad (14)$$

Global fits at the moment imply [21]

$$N_\nu^{\text{CMB}} \approx 3 \pm 2 \quad (15)$$

somewhat depending on which priors and on which data are included in the fit. Future data might allow a better discrimination.

3.1 Results

The results are collected in Fig. 3. **We plot** the effective numbers N_ν of neutrinos which translate the physical observables (the ${}^4\text{He}$ and D abundances and the energy density in neutrinos at recombination), as dictated by eqs. (8) and eq. (14), and the value of the quantity $\Omega_\nu h^2$, defined by eq. (10). We shade the regions that correspond to $Y_p \gtrsim 0.26$ (i.e. $N_\nu^{4\text{He}} > 3.8$) or $\Omega_\nu h^2 > 10^{-2}$ and are therefore ‘strongly disfavoured’ or ‘excluded’ (depending on how conservatively one estimates systematic uncertainties) within minimal cosmology. The other lines indicate the sensitivity that future experiments might reach.

In order to **qualitatively understand** these precisely computed results, it is useful to begin with the case of mixing with a matter eigenstate $\nu_{1,2,3}$ (upper row of Fig. 3), and to consider first the line which corresponds to N_ν^{CMB} (blue dashed line): indeed, this quantity is sensitive only to the total number of neutrinos, and not to the specific flavor (ν_e , ν_μ or ν_τ) which mixes with ν_s . In the region above the lines, the production of sterile neutrinos via oscillations is efficient and populates to some extent the sterile species. The slope of the lines can be reproduced by simple analytical estimates [12], and is also intuitive: loosely speaking, at small Δm^2 the production starts late

⁴⁾Actually, the naive N_ν discussed at the beginning of the Section is usually defined as equal to this N_ν^{CMB} . It should be clear from the above discussion that, instead, $N_\nu^{4\text{He}}$ and N_ν^{D} stand for two other different quantities. The three of them come to coincide only in the limiting case in which the only effect of the extra degrees of freedom is a contribution in the total energy density.

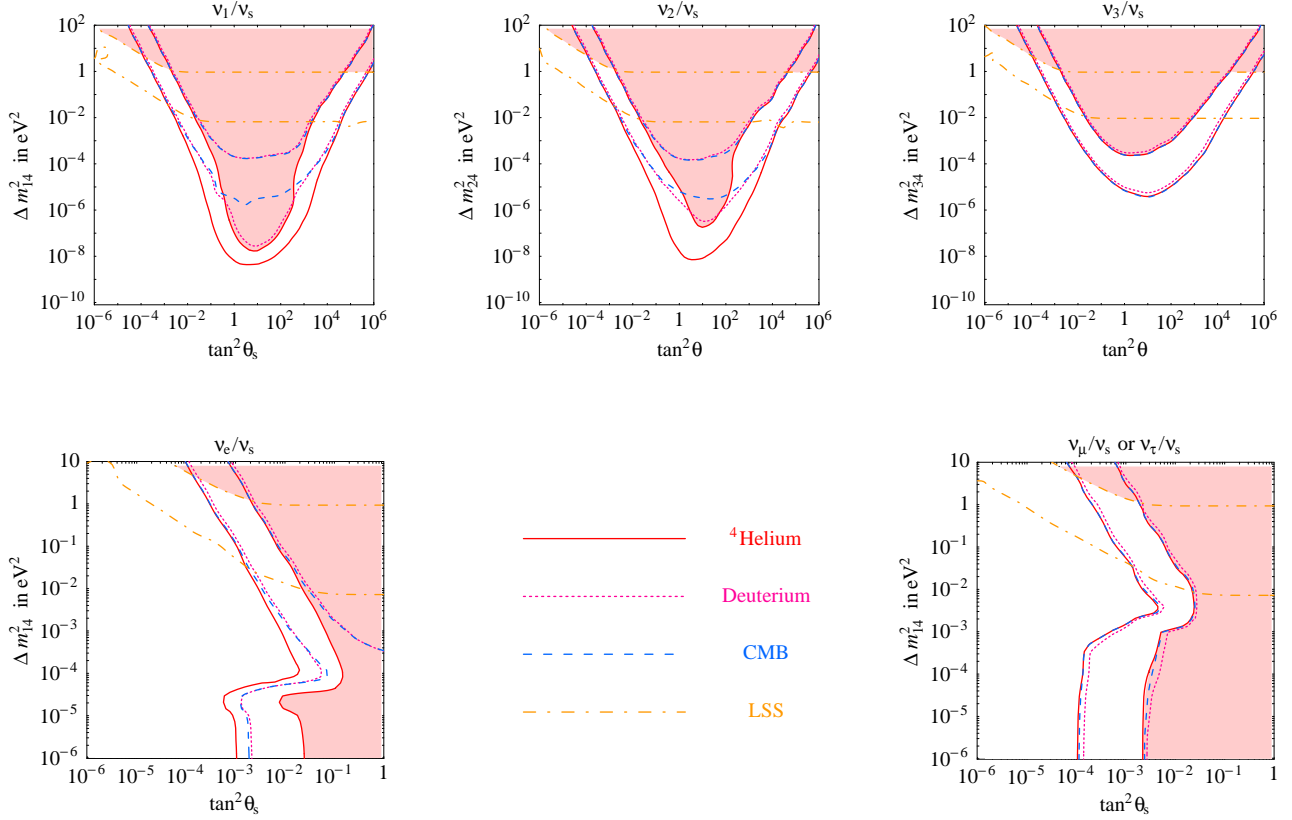


Figure 3: Cosmological effects of sterile neutrino oscillations. We collect four different signals. *The continuous red line refers to the ${}^4\text{He}$ abundance* (we shaded as ‘strongly disfavoured’ the regions where its value corresponds to $N_\nu^{4\text{He}} > 3.8$ i.e. $Y_p \gtrsim 0.26$), *the purple dotted line to the deuterium abundance*, and *the dashed blue line to the effective number of neutrinos at recombination*. We plotted isolines of these three signals corresponding to an effective number of neutrinos $N_\nu = 3.2$ and 3.8 . The precise meaning of the parameter N_ν in the three cases is explained in the text. *The upper (lower) dot-dashed orange lines corresponds to $\Omega_\nu h^2 = 10^{-2}$ (10^{-3})*; we shaded as ‘strongly disfavoured’ by the data the regions where $\Omega_\nu h^2 > 10^{-2}$.

and needs a large mixing angle to be efficient enough; at large Δm^2 , on the contrary, even a small mixing angle (i.e. a small rate of production) gives rise to a significant amount. Effects are larger at $\theta_s > \pi/4$ (i.e. $\tan \theta_s > 1$) because this corresponds to having a mostly sterile state lighter than the mostly active state, giving rise to MSW resonances (both in the neutrinos and anti-neutrinos channels).

In the region of $\Delta m^2 \lesssim 10^{-5} \text{ eV}^2$, the production starts *too* late, namely after neutrino freeze-out. The only effect of the oscillations is then to redistribute the energy density between the active and sterile species, keeping the total entropy constant (there can be no “refill” from the thermal bath) so the bound on N_ν^{CMB} does not apply.

Let us then move to discuss the BBN probes (${}^4\text{He}$ and D abundances): at large Δm^2 their isolines essentially coincide with N_ν^{CMB} . On the contrary, in the region of $\Delta m^2 \lesssim 10^{-5} \text{ eV}^2$, if $\nu_e \rightarrow \nu_s$ oscillations occur then ν_s are created by depleting ν_e , as just discussed. Thus the n/p ratio is affected and consequently the ${}^4\text{He}$ abundance and, to a lesser extent, the D abundance. This is apparent in the ν_1/ν_s and ν_2/ν_s plots of fig. 3, where the bound extends in the lower part. The bound is stronger for the eigenstate which contains the larger portion of electron flavor: ν_1 . In the case of ν_3/ν_s mixing nothing happens because no significant ν_e component is present in ν_3 , as θ_{13} is very small.

In turn, for $\Delta m^2 \lesssim 10^{-8} \text{ eV}^2$ oscillations begin *really too* late, namely even after the decoupling of $n \leftrightarrow p$ reactions. At that stage, the relative n/p abundance is no more affected by the neutrino populations (but only by neutron decay), so no bounds apply.

The mixing with flavor eigenstates ν_e, ν_μ, ν_τ (lower row of Fig. 3) is qualitatively different, for the general reasons

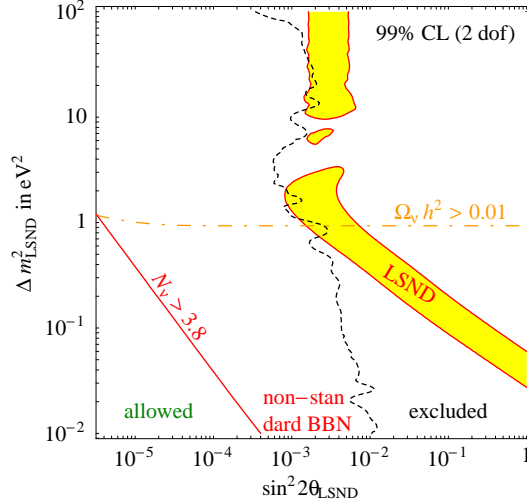


Figure 4: The LSND anomaly interpreted as oscillations of 3+1 neutrinos versus the cosmological constraints. *Shaded region: suggested at 99% C.L. by LSND. Black dotted line: 99% C.L. global constraint from other neutrino experiments (mainly Karmen, Bugey, SK, CDHS). Continuous red line: the bound from BBN corresponding to $Y_p \simeq 0.26$, i.e. $N_\nu = 3.8$ thermalized neutrinos. Dot-dashed orange line: the bound from LSS corresponding to $\Omega_\nu h^2 = 0.01$.*

explained in section 2. Essentially, since the flavor eigenstate is spread on two or three mass eigenstates, the active \rightarrow sterile oscillations occur at two or three different Δm^2 , of which one is always large enough to give an effect for every Δm^2_{14} (our variable of choice for the vertical axis).

In the case of ν_e/ν_s mixing, we see the effect of the solar mass splitting as a bump in the corresponding panel in fig. 3: if the (mainly) sterile state lies below ν_2 , the $\Delta m^2_{\text{sun}} \sim 7 \cdot 10^{-5} \text{ eV}^2$ becomes the dominant mass difference.⁵⁾ The bounds then approximate to vertical lines and they are stronger in $\tan \theta_s$ because of the resonant disposition. More precisely, this is true for the moderate effect expressed by the $N_\nu = 3.2$ line; Δm^2_{sun} is sufficient to cause a more incisive effect ($N_\nu = 3.8$ or more) only in the case of ${}^4\text{He}$.

In the case of $\nu_{\mu,\tau}/\nu_s$ mixing, the Δm^2_{atm} plays exactly the same role, and this time it is large enough to affect all probes.

Finally, the LSS structure bound on $\Omega_\nu h^2$ consists of an horizontal line in the central part of the plots: qualitatively, as long as the sterile species is fully populated it is its contribution to the sum of the masses (i.e. the Δm^2) which is bounded from above. The constraints get weaker for very small $\tan \theta_s$, where the sterile neutrinos are less efficiently produced ($\rho_{\nu_s} \ll$). At $\tan \theta_s > 1$ the bound from Ω_ν holds even for very small mixing, $\theta_s \simeq \pi/2$, just because this region corresponds to heavy active neutrinos.

In summary, fig. 3 displays the excluded, the allowed and the future testable regions of the active/sterile mixing parameter space, for six limiting cases, for what concerns cosmological probes. Any specific model of a sterile neutrino identifies a preferred point (or area) in one of these spaces or in a suitable combination of them, and should therefore be tested on them. This is what we do, as an example, for the LSND sterile neutrino in the next Section.

3.2 LSND: in or out?

The LSND experiment reports a signal [6] for $\bar{\nu}_\mu \rightarrow \bar{\nu}_e$ oscillations in the appearance of $\bar{\nu}_e$ in an originally $\bar{\nu}_\mu$ beam. The best fit point is located at $\sin^2 \theta_{\text{LSND}} = 3 \cdot 10^{-3}$, $\Delta m^2_{\text{LSND}} = 1.2 \text{ eV}^2$ (the whole allowed region is represented in fig. 4).

The “3+1 sterile” neutrino explanation assumes that the $\bar{\nu}_\mu \rightarrow \bar{\nu}_e$ oscillation proceeds through $\bar{\nu}_\mu \rightarrow \bar{\nu}_s \rightarrow \bar{\nu}_e$. The large LSND mass scale Δm^2_{LSND} separates the three active states (split by the solar and atmospheric gaps) from the additional sterile state. The effective angle of the LSND oscillation θ_{LSND} can be expressed in terms of

⁵⁾ Keep in mind that we are assuming a negligible θ_{13} so there is no electron component in the third mass eigenstates which can feel the mixing with the sterile neutrino. That’s why Δm^2_{atm} has no role in this case.

the two active-sterile angles $\theta_{es}, \theta_{\mu s}$ as $\theta_{\text{LSND}} \approx \theta_{es} \cdot \theta_{\mu s}$.⁶⁾ However, each one of these two angles is constrained by several other experiments that found no evidence of electron or muon neutrino disappearance. Moreover, the $\bar{\nu}_\mu \rightarrow \bar{\nu}_e$ oscillations are directly excluded by KARMEN in a fraction of the parameter space. As a result [22], a large portion, but not the totality, of the area indicated by the LSND experiment is ruled out (see fig. 4). The poor compatibility with solar and atmospheric oscillation data, in the context of four ν mixing, also puts the LSND sterile neutrino in a difficult position [23].

How does the LSND signal compare to the cosmological bounds discussed above? Fig. 4 shows the constraints from BBN and from LSS superimposed to the LSND region⁷⁾. We see that **the entire LSND region is ruled out by the BBN constraint**: basically, for every value of its mixing parameters the LSND sterile neutrino completely thermalizes and implies an unacceptable modification of the ${}^4\text{He}$ primordial abundance. Of course, remember that allowing non-standard modifications to cosmology/BBN has the power to relax the bound to some extent. Exemplar is the case of a large primordial neutrino asymmetry, as discussed above. Other recent suggestions include [24].

The constraint on Ω_ν is well approximated by the horizontal line corresponding to $\Omega_\nu h^2 = m_4/93.5 \text{ eV}$. It starts to bend (as discussed in Sec.3.1) only at smaller values of the effective θ_{LSND} mixing angle.

Fig. 4, that combines the precise computation of the evolution of mixed neutrinos in the Early Universe and of the neutrino experimental data, therefore reproduces and completes the estimates already presented in [25] and [26].

4 Sterile Neutrinos in Supernova sauce

Generalities: Supernovæ can be powerful and important laboratories for neutrino physics, and therefore in particular for the physics of sterile neutrinos. The fundamental reasons for this basic fact are simply listed:

- SNe are abundant sources of neutrinos, since this is the main channel into which most of their enormous energy is emitted; as a consequence, neutrinos play a crucial role in the evolution of the SN phenomenon;
- given the characteristic temperatures of the SN environment, the typical energy of the emitted neutrinos ($\sim 10 \div 20 \text{ MeV}$) is such that they can be easily detected on Earth;
- SNe are so far away that neutrinos must travel over distances so large that they have plenty of time (or space) to experience and fully develop the consequences of several “exotic” effects (oscillations, non-conventional very feeble interactions, decay...), if any is present;
- SN cores are so extremely dense that neutrinos remain trapped and undergo matter effects that cannot be relevant anywhere else.

On the other hand, it is true that the physics of supernovæ is very complicated and demanding, and could pose a threat on their possible usefulness as “clean experiments”. Nevertheless, the basic features are robust enough to be used as incontrovertible criteria, sometimes, maybe, requiring a sensible compromise between detailness and usefulness in the treatment of SN physics. At the present epoch, the twenty-something events of the SN1987a signal [27] already allow to set cautious constraints. The future is however brighter: running solar neutrino experiments could detect thousands of events from a future SN exploding at distance $D \sim 10 \text{ kpc}$ and an even more impressive harvest of data could come from a future Mton water-Čerenkov detector or from other more SN-oriented future projects [28], making the quantitative analysis of the SN neutrinos worthwhile for the search of sterile states. Previous analysis have investigated the subject [29].

Neutrino evolution: What we need to do is simply said: we must follow the fate of the neutrinos emitted from neutrino-spheres⁸⁾ along their travel through the star mantle, the vacuum and (possibly) the Earth.⁹⁾ The existence of the sterile neutrino can introduce modifications at each of these steps, via matter or vacuum conversions, in different ways for each possible choice of the sterile mixing parameters.

⁶⁾In our parameterization, this simply corresponds to a unit vector $\vec{n} = (n_e, n_\mu, n_\tau) \simeq (\frac{1}{\sqrt{2}}, \frac{1}{\sqrt{2}}, 0)$.

⁷⁾In constructing fig. 4 the BBN constraint has been minimized setting $\theta_{es} \approx \theta_{\mu s} \approx \theta_{\text{LSND}}$, when this is allowed by the neutrino disappearance data.

⁸⁾Neutrino-sphere: the region of the star mantle at which the density becomes low enough that neutrinos (produced in the core) are no more trapped and freely stream outwards.

⁹⁾For the range of $\Delta m_s^2 \lesssim \text{few eV}$ to which we are confined by the cosmological bounds discussed in Sec.3, the MSW resonances with the sterile state occur out of the neutrino-sphere. The resonances would enter in the neutrino-spheres (in the inner core) for $\Delta m_s^2 \gtrsim 10^5 \text{ eV}^2$ ($\gtrsim 10^7 \text{ eV}^2$ respectively).

In more detail: one has to follow the evolution of the 4×4 neutrino density matrix ϱ_m , written in the basis of instantaneous mass eigenstates. For instance, a ν_e with energy E_ν is described by $\varrho_m = V_m^\dagger \cdot \text{diag}(1, 0, 0, 0) \cdot V_m$ where V_m depends on E_ν and, in general, on the position in the star. The mixing matrices in matter (V_m) and vacuum (V) are computed diagonalizing the Hamiltonian

$$\mathcal{H} = \frac{1}{2E_\nu} \left[V \text{diag}(m_1^2, m_2^2, m_3^2, m_4^2) V^\dagger + E_\nu \text{diag}(V_e, V_\mu, V_\tau, 0) \right] \quad (16)$$

and ordering the eigenstates according to their eigenvalues $H_i \equiv m_{\nu_{m_i}}^2/2E_\nu$: ν_{m1} (ν_{m4}) is the lightest (heaviest) neutrino mass eigenstate in matter. The evolution up to the detection point is described by a 4×4 unitary evolution matrix \mathcal{U} so that at detection point the density matrix ϱ in the basis of flavor eigenstates is

$$\varrho = V \cdot \mathcal{U} \cdot \varrho_m(E_\nu) \cdot \mathcal{U}^\dagger \cdot V^\dagger \quad \text{with} \quad \mathcal{U} = \mathcal{U}_{\text{Earth}} \cdot \mathcal{U}_{\text{vacuum}} \cdot \mathcal{U}_{\text{star}}. \quad (17)$$

The evolution in vacuum is simply given by $\mathcal{U}_{\text{vacuum}} = \text{diag} \exp(-iLm_{\nu_i}^2/2E_\nu)$. Combined with average over neutrino energy it suppresses the off-diagonal element ϱ_m^{ij} when the phase differences among eigenstates i and j are large.

The evolution in the matter of the star is more complicated because several level crossings can occur, say at radii $r_1 \dots r_N$. At each one of them, there is a certain ‘‘jump’’ probability. In the present formalism, this can be expressed by a 4×4 rotation matrix P , with the rotation angle given by $\tan^2 \alpha = P_C/(1 - P_C)$ where P_C is the level crossing probability. Indeed, in particular, when levels i and j cross in an adiabatic way, $P = \mathbb{I}$. If instead the level crossing is fully non adiabatic P is a rotation with angle $\alpha = 90^\circ$ in the (ij) plane.

The computation of P_C at the crossings requires attention. Focussing e.g. on $\theta_s < \pi/4$, at a crossing between a mainly active state ν_a and the mainly sterile state ν_s we compute it as

$$P_C = \frac{e^{\tilde{\gamma} \cos^2 \theta_{as}^m} - 1}{e^{\tilde{\gamma}} - 1} \quad \gamma = \frac{4\mathcal{H}_{as}^2}{d\mathcal{H}_a/dr} \equiv \tilde{\gamma} \cdot \frac{\sin^2 2\theta_{as}^m}{2\pi |\cos 2\theta_{as}^m|} \quad \text{where} \quad \sin \theta_{as}^m = \vec{n} \cdot \vec{\nu}_a^m \sin \theta_s. \quad (18)$$

where it is important to notice that γ and θ_{as}^m must be computed around the resonance, where $\mathcal{H}_{aa} = \mathcal{H}_{ss}$ (or around the point where adiabaticity is maximally violated, in cases where there is no resonance) and are in general different from their vacuum values (that are instead conveniently used to parameterize P_C in the simpler 2ν case). [30]

Between a level crossing and the following one the evolution proceeds as governed by the matter Hamiltonian, so that the complete form for $\mathcal{U}_{\text{star}}$ is

$$\mathcal{U}_{\text{star}} = P_{r_n} \dots P_{r_2} \cdot \text{diag} \exp \left(-i \int_{r_1}^{r_2} ds \frac{m_{\nu_{mi}}^2}{2E_\nu} \right) \cdot P_{r_1} \cdot \text{diag} \exp \left(-i \int_{r_0}^{r_1} ds \frac{m_{\nu_{mi}}^2}{2E_\nu} \right). \quad (19)$$

In practice, given the importance of the matter effects in the star mantle and the very long baseline to Earth, the evolution between the level crossings and in vacuum averages to zero the off-diagonal elements that are possibly produced by the rotation matrices, introducing significant simplifications. However, if two states have $\Delta m^2 \lesssim 10^{-18} \text{ eV}^2$ vacuum oscillations do not give large phases: evolution in the outer region of the SN and in vacuum must be described keeping the off-diagonal components of the density matrix.

Finally, for simplicity we now assume that the neutrinos do not travel through the Earth matter, so that $\mathcal{U}_{\text{Earth}}$ is trivial. In the case of the SN1987a signal, this was not true but disregarding it only implies a few percent error, well within the general uncertainties for our purposes. In the case of the next SN event, it could be in general reintroduced.

Having described the general formalism, let us now focus more closely on the peculiarities of the SN case. At the neutrinosphere, matter effects are dominant, so that matter eigenstates coincide with flavor eigenstates (up to a trivial permutation dictated by the MSW potentials that will be more clear below): the initial density matrix consists of $\varrho_m = \text{diag}(\Phi_{\nu_s}^0, \Phi_{\nu_e}^0, \Phi_{\nu_\tau}^0, \Phi_{\nu_\mu}^0)/\Phi_{\text{tot}}^0$, where Φ_ν^0 are the flavor fluxes from the neutrinosphere and Φ_{tot}^0 stands for their sum. The final fluxes at the detection point will be then given by the diagonal entries of ϱ of eq. (17): $(\Phi_{\nu_e}, \Phi_{\nu_\mu}, \Phi_{\nu_\tau}, \Phi_{\nu_s}) = \text{diag}(\varrho) \cdot \Phi_{\text{tot}}^0$.

Concerning the initial fluxes, the accurate results of simulations are usually empirically approximated by a Fermi-Dirac spectrum for each flavor $\nu_e, \bar{\nu}_e, \nu_x$ (ν_x collectively denotes $\nu_{\mu, \tau}, \bar{\nu}_{\mu, \tau}$), with a ‘‘pinching’’ that slightly suppresses the low energy portion and the high energy tail. Based on the recent results of [31], we adopt the following average energies and total luminosities for the various neutrino components at the time of the snapshot of fig. 5 (see below): $\langle E_{\nu_e, \bar{\nu}_e, \nu_x} \rangle \simeq 12, 14, 14 \text{ MeV}$, $L_{\nu_e, \bar{\nu}_e, \nu_x} \simeq 30, 30, 20 \cdot 10^{51} \text{ erg sec}^{-1}$, assuming (in accordance with numerical calculations) that the ratios of luminosities do not vary much during the whole emission. The initial flux of sterile neutrinos is assumed to be vanishing, as a consequence of the fact that matter oscillations only take place out of the neutrinosphere.

The MSW potentials of eq. (16), experienced by the neutrinos in SN matter are

$$\begin{aligned} V_e &= \sqrt{2}G_F n_B (3Y_e - 1)/2, & V_\tau &= V_\mu + V_{\mu\tau}, \\ V_\mu &= \sqrt{2}G_F n_B (Y_e - 1)/2, & V_s &= 0, \end{aligned} \quad (20)$$

where n_B is the baryon number density ($n_B = \rho(r)/m_N$ where $m_N \approx 939 \text{ MeV}$ is the nucleon mass) and $Y_e = (N_{e^-} - N_{e^+})/n_B$ is the electron fraction per baryon. Antineutrinos experience the same potentials with opposite sign. The difference $V_{\mu\tau}$ in the ν_μ and ν_τ potentials, which appears at one loop level due to the different masses of the muon and tau leptons [33], is, according to the SM

$$V_{\mu\tau} = \frac{3G_F^2 m_\tau^2}{2\pi^2} \left[2(n_p + n_n) \ln \left(\frac{M_W}{m_\tau} \right) - n_p - \frac{2}{3}n_n \right]. \quad (21)$$

The effect is not irrelevant in the inner dense regions: for densities above $\rho \sim 10^8 \text{ g cm}^{-3}$, the $\mu\tau$ vacuum mixing is suppressed.

A crucial point concerns the characteristic of the matter density $\rho(r)$ and of the electron fraction Y_e in the mantle of the star. We adopt the profiles represented in fig. 5 and we model them with analytic functions that preserve their main features. Namely, the density profile decreases according to a power law r^{-4} out of the $\sim 10 \text{ km}$ inner core (where instead it has a roughly constant, nuclear density value). At much larger distances the density profile gets modified in a time-dependent way by the passage of the shock wave. Present simulations have difficulties in reproducing this phenomenon and therefore cannot reliably predict the density profile in the outer region. Therefore for $r \gtrsim 500 \text{ km}$ we assume a power law $\rho(r) = 1.5 \cdot 10^4 (R_\odot/r)^3 \text{ g/cm}^3$, which roughly describes the static progenitor star.

In turn, the peculiar Y_e profile in fig. 5 is inevitably dictated by the deleptonization process: behind the shock wave which has passed in the mantle matter, the electron capture on the newly liberated protons is rapid, driving Y_e to low values ($\sim 1/4$). In the outer region, where the density is sensibly lower, the efficiency of the capture is much lower, so that Y_e essentially maintains the value $\sim 1/2$ typical of normal

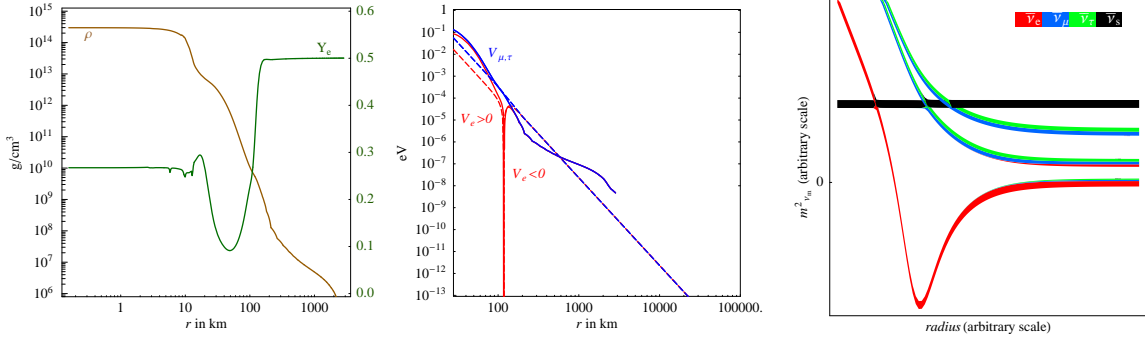


Figure 5: Inside the supernova. *Left panel: Density $\rho(r)$ and electron fraction $Y_e(r)$ from [32]. Center panel: matter potentials for $\bar{\nu}_e$ (red solid line) and for $\bar{\nu}_{\mu,\tau}$ (blue solid line); the dashed lines are the analytic modelization that we adopt. Right panel: a representation of the antineutrino matter eigenstates with their flavor content, as functions of the radius in the interior of the SN; the drawing is made in the specific case of small ν_e/ν_s mixing and large $\Delta m_{14}^2 (> \Delta m_{\text{atm}}^2)$ for the sake of illustration; we are assuming small θ_{13} and normal hierarchy.*

matter.¹⁰⁾ This is important because the matter potential V_e of electron (anti)neutrinos flips sign, see eq. (20), when, in the deep region of the mantle Y_e steeply decreases below $1/3$.

The knowledge of the matter potentials (and of the neutrino masses and mixings) allows to draw the pattern of the (anti-)neutrino eigenstates with their flavor content, as functions of the radius r in the interior of the star. This is represented in the right panel of fig. 5, in the specific case of small ν_e/ν_s mixing and large $\Delta m_s^2 (\gg \Delta m_{\text{atm}}^2)$ for the sake of illustration.

In the end, we collect the modified (anti)neutrino fluxes and deduce the modifications to some relevant observables; in particular, we focus on the final flux of $\bar{\nu}_e$, which are best detected through $\bar{\nu}_e p \rightarrow e^+ n$ at the Čerenkov detectors.

4.1 Results

The results are collected in fig. 6, where we plot the reduction of the $\bar{\nu}_e$ event rate in a typical Čerenkov detector due to sterile mixing¹¹⁾, and in fig. 7, where we plot the modified average energy and the distortion of the $\bar{\nu}_e$ spectrum for a few specific choices of mixing parameters.

In order to **understand qualitatively** the main features of these results it is useful to look at the pattern of level crossings, like the one qualitatively depicted in fig. 5. Indeed, as discussed above, the **active/sterile MSW resonances** in the matter of the star are the crucial places where the neutrino flux is non-trivially modified, the rest is simply vacuum oscillations. There are three possible resonances:

1. The mostly $\bar{\nu}_s$ eigenstate crosses the mostly $\bar{\nu}_e$ eigenstate at $r \sim 100$ km, where V_e flips sign. At this point matter effects dominate over active neutrino masses, so that active mass eigenstates coincide with flavor eigenstates. Since V_e flips sign in a steep way this resonance is effective only if $\Delta m_{14}^2 \gtrsim 10^{-1 \div 0} \text{ eV}^2$ (different SN simulations gives values in this range).
2. If the mostly sterile eigenstate is the lightest one (in our parameterization this needs $\theta_s \gtrsim \pi/4$) the two eigenstates in 1. cross again at larger r . Pictorially, this second resonance is present when the sterile black line is lowered below the others in fig. 5. This MSW resonance occurs at large r where V_e is smooth, so that it is effective down to $\Delta m_{14}^2 \gtrsim 10^{-6 \div 8} \text{ eV}^2$. Again, the significant uncertainty is due to uncertainties on the SN density gradient.
3. When the mostly sterile eigenstate is the heaviest or the next-to-heaviest state, it also crosses one or both of two mostly $\bar{\nu}_{\mu,\tau}$ eigenstates. This is the case illustrated in fig. 5. The values of Δm_{24}^2 and Δm_{34}^2 determine at which r these crossings takes place, and consequently the flavor composition of the mostly active states at the resonance. Entering in the SN, the small $\bar{\nu}_e$ component of $\bar{\nu}_{2,3}^m$ disappears as soon as $V_e - V_\mu$ dominates over Δm_{sun}^2 . In any case, active/sterile MSW resonances with the mostly $\bar{\nu}_{\mu,\tau}$ states affect only marginally the $\bar{\nu}_e$ rate, right because the $\nu_{2,3}^m$ contribution to $\bar{\nu}_e$ is secondary.

¹⁰⁾The data refer to ~ 0.3 sec after bounce for a typical star of ~ 11 solar masses. The subsequent evolution is supposed to move the wave of the Y_e profile slightly outwards, maintaining, however, its characteristic shape.

¹¹⁾We focus on $\bar{\nu}_e p$ scatterings with the cuts and efficiency of the KamiokandeII experiment. The cross section is taken from [34].

At each of the resonances, part of the neutrino flux can then convert into the sterile state and deplete the final active flavors. Combinations of more than one resonance can occur, depending on the mixing parameters. These considerations allow to understand the regions of $\bar{\nu}_e$ **flux reduction** in fig. 6.

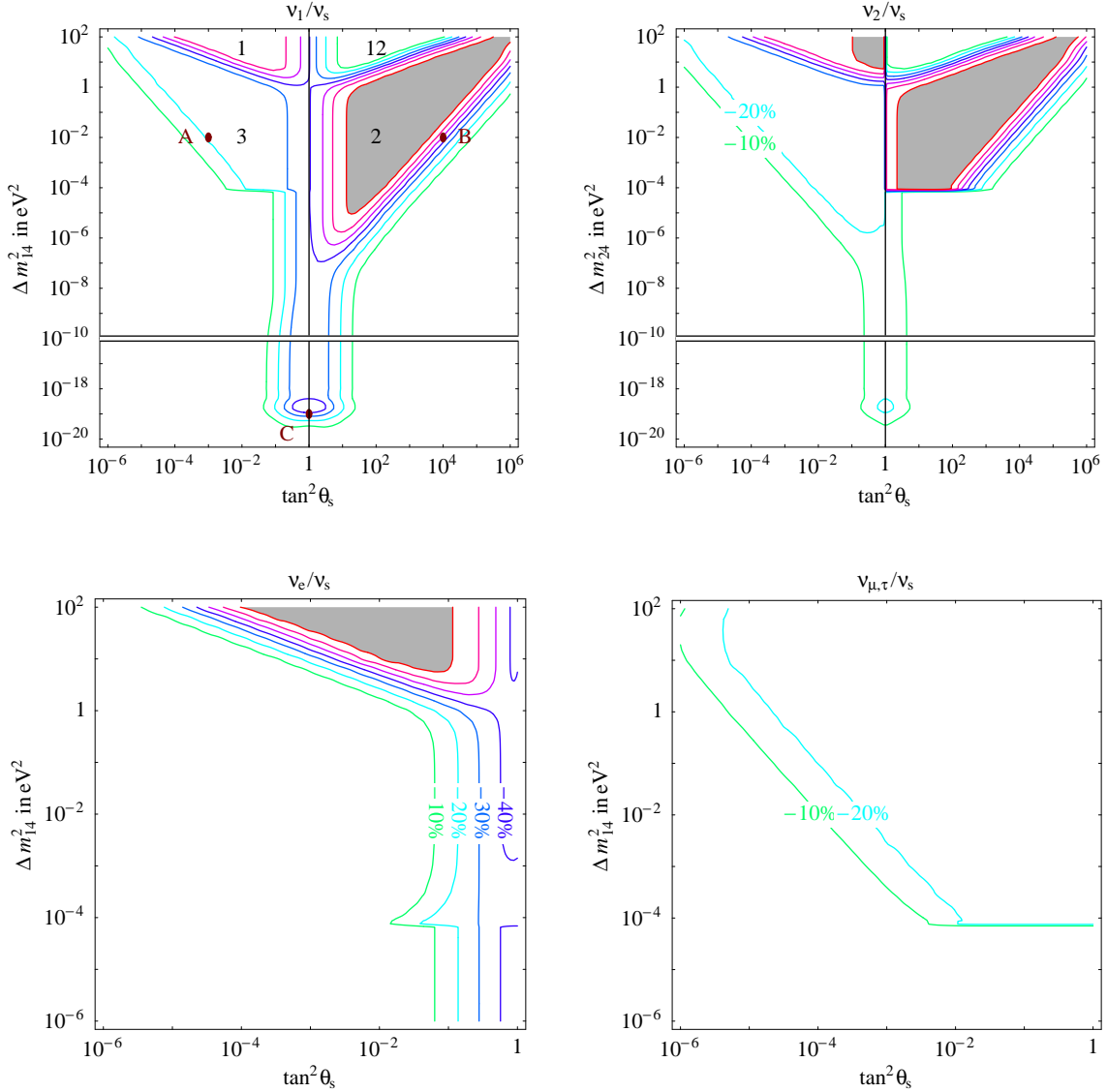


Figure 6: Sterile effects in supernovæ. The iso-contours correspond to a 10, 20, 30, 40, 50, 60, 70 % deficit of the SN $\bar{\nu}_e$ total rate due to oscillations into sterile neutrinos. The deficit is measured with respect to the rate in absence of active/sterile oscillations but of course in presence of active/active oscillations (which reduce the unrealistic no-oscillation-at-all rate by $\sim 10\%$). We shaded as disfavoured by SN1987a data regions with a deficit larger than 70%. While the qualitative pattern is robust, regions with MSW resonances can shift by one order of magnitude in Δm^2 using different SN density profiles. $\bar{\nu}_3/\bar{\nu}_s$ mixing (not plotted) does not give significant effects. Fig. 7 studies in detail the sample points here marked as A, B, C, and the regions 1, 2, 12, 3 are discussed in the text.

Let us start from the case of ν_1/ν_s mixing. Resonance 1 gives a sizable reduction in region 1 and resonance 2 gives a sizable reduction in region 2. Had we ignored solar mixing the maximal deficit would have been 100%, while in presence of solar oscillations the maximal effect is a $\sim 80\%$ deficit. More precisely, in the interior of region 1 one obtains $\Phi_{\bar{\nu}_e} = \sin^2 \theta_{\text{sun}} \Phi_{\bar{\nu}_e}^0$ because resonances 1 and 3 are fully adiabatic. In the interior of region 2 one obtains $\Phi_{\bar{\nu}_e} = \sin^2 \theta_{\text{sun}} \Phi_{\bar{\nu}_{\mu,\tau}}^0$ because resonance 2 is fully adiabatic and resonance 1 irrelevant. Therefore, given the assumed initial fluxes, the $\bar{\nu}_e$ rate gets reduced slightly more strongly in region 2 than in region 1.

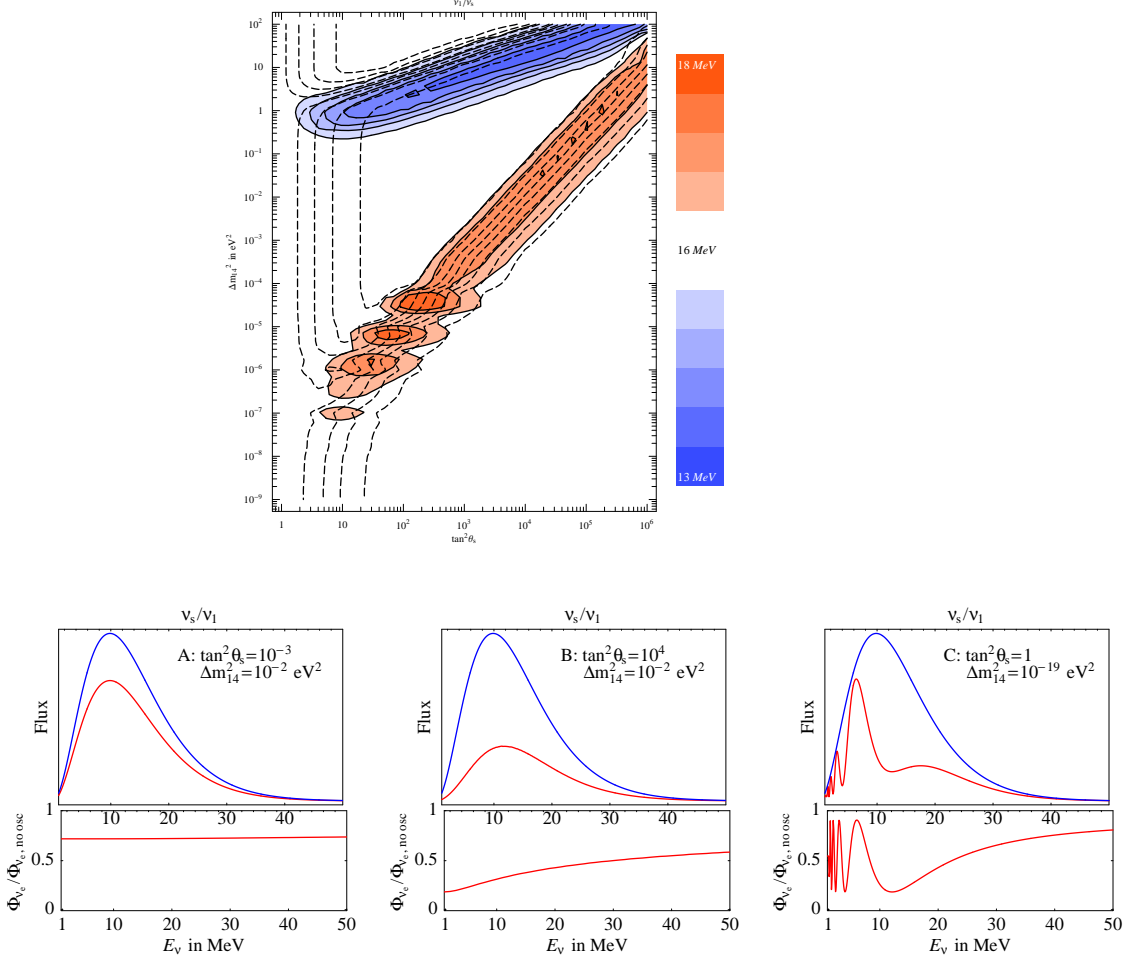


Figure 7: Sterile effects in supernovae. Average $\bar{\nu}_e$ energy in the ν_1/ν_s plane ($\tan^2 \theta_s > 1$ portion) and distortion of the $\bar{\nu}_e$ flux at sample points A, B, C.

In region 12 both resonances 1 and 2 are effective, and tend to compensate among each other: resonance 1 converts $\bar{\nu}_e$ into $\bar{\nu}_s$ and resonance 2 reconverts $\bar{\nu}_s$ into $\bar{\nu}_e$.

In region 3, resonance 3 gives a 20% suppression of the $\bar{\nu}_e$ rate, that sharply terminates when $\Delta m_{14}^2 < \Delta m_{\text{sun}}^2$. This is due to a strong suppression of the mostly $\bar{\nu}_{\mu,\tau}$ eigenstates, which due to solar oscillations would give a 20% contribution to the $\bar{\nu}_e$ rate (ignoring solar mixing, there would be no suppression of the $\bar{\nu}_e$ rate in region 3). This reduction of the $\bar{\nu}_{\mu,\tau}$ fluxes induced by resonances 3 could be better probed by measuring the NC rate (which gets a $\lesssim 40\%$ reduction) and, if neutrinos cross the Earth, by distortions of the $\bar{\nu}_e$ energy spectrum.

The tail at smaller Δm^2 and around maximal mixing is due to vacuum oscillations, that can reduce the $\bar{\nu}_e$ rate by $\lesssim 50\%$: their effect persists down to $\Delta m^2 \sim E_{\nu}/D \sim 10^{-18} \text{ eV}^2$. The precise value depends on the distance D (we assumed $D = 10 \text{ kpc}$).

The other mixing cases are understood in similar ways. We remind that our parametrization is discontinuous at $\theta_s = \pi/4$: this is reflected in the panel of fig. 6 which illustrates ν_2/ν_s mixing. Resonance 2 sharply terminates when $\Delta m_{24}^2 < \Delta m_{\text{sun}}^2$. Except for these differences, this case is quite similar to the previous one, because $\bar{\nu}_1$ and $\bar{\nu}_2$ get strongly mixed by matter effects. On the contrary ν_3/ν_s mixing (not shown) does not give a significant reduction of the $\bar{\nu}_e$ rate.

Mixing with the flavor eigenstates behaves in a similar way. Namely, the $\nu_{\mu,\tau}/\nu_s$ figure shows the reduction in region 3 due to resonances 3, and the ν_e/ν_s figure shows the reduction in region 1 due to resonance 1. The additional feature at $\Delta m_{14}^2 \sim \Delta m_{\text{sun}}^2$ is due to adiabatic conversion (for large sterile angles) between the mostly-sterile state and ν_2 , that are almost degenerate in this condition. For larger Δm_{14}^2 , there is no $\bar{\nu}_e$ component in $\bar{\nu}_2^m$ so that the crossing is totally non adiabatic, while for smaller Δm_{14}^2 the two states are separated. Sterile effects persists at all values of Δm_{14}^2 , even if it is small.

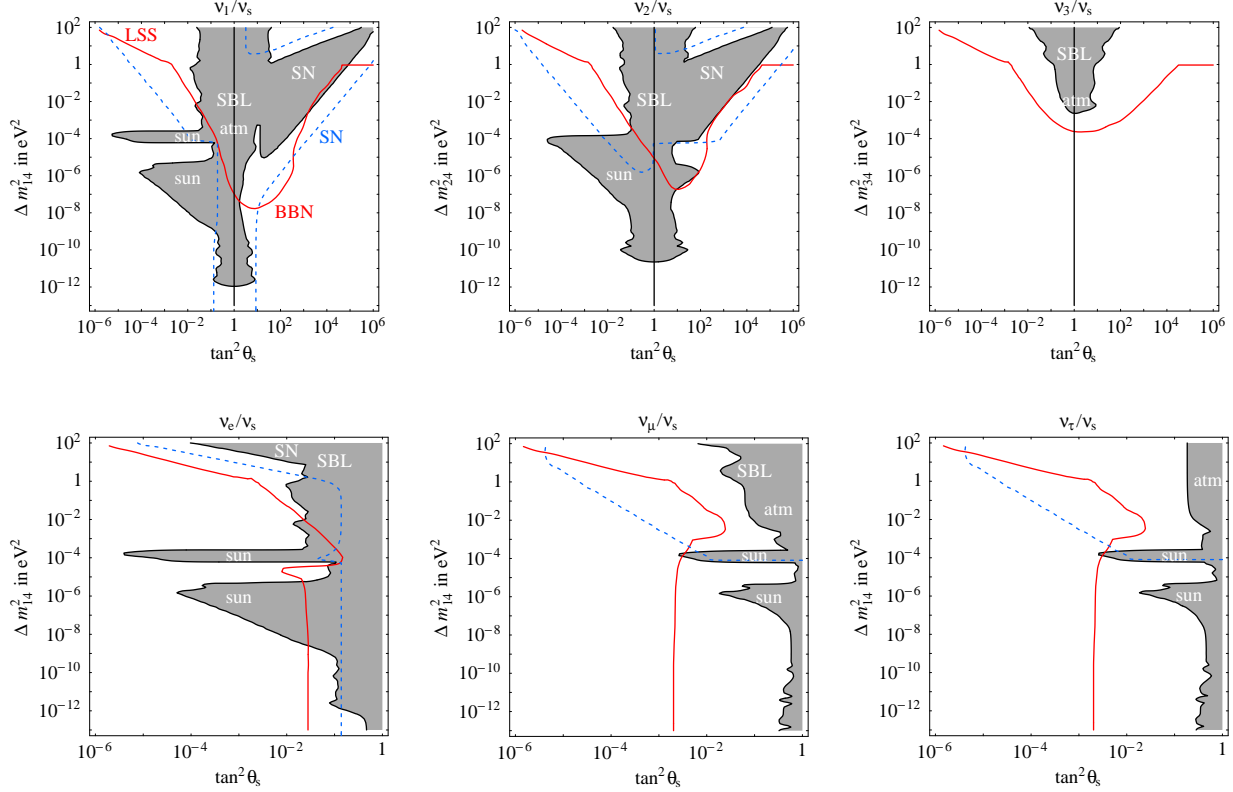


Figure 8: Summary of sterile neutrino effects. *The shaded region is excluded at 99% C.L. (2 dof) by solar or atmospheric or reactor or short base-line experiments. We shaded as excluded also regions where sterile neutrinos suppress the SN1987A $\bar{\nu}_e$ rate by more than 70%. This rate is suppressed by more than 20% inside the dashed blue line, that can be explored at the next SN explosion if it will be possible to understand the collapse well enough. Within standard cosmology, the region above the red continuous line is disfavoured (maybe already excluded) by BBN and LSS.*

The reductions highlighted in fig. 6 have to be compared to the measured flux to set constraints and identify anomalies. This will certainly be fruitful in the future. At present, however, the theoretical uncertainties on the SN evolution and fluxes and the smallness of the SN1987a data set only allow to put conservative constraints: we simply shaded as ‘disfavoured’ regions where sterile effects reduce the $\bar{\nu}_e$ rate by more than 70%.

In the same perspective, important observables in the future SN event will be the $\bar{\nu}_e$ **spectrum**, where distortions could be induced by sterile oscillations, or more generally the **average $\bar{\nu}_e$ energy**. In absence of sterile oscillations we expect $\langle E_{\bar{\nu}_e} \rangle \approx 15$ MeV with a quasi-thermal spectrum. In presence of sterile oscillations, these observables can be affected in selected regions of the parameter space, as illustrated by figure 7. The average energy can increase up to $\langle E_{\bar{\nu}_e} \rangle \approx 18$ MeV and decrease down to ≈ 12 MeV along the sides of the MSW triangle. The distorted spectrum which correspond to the first case is plotted in fig. 7B. Vacuum oscillations can also give well known distortions, as exemplified in fig. 7C. These effects seem larger than experimental and theoretical uncertainties. In all other cases sterile effects give a quasi-energy-independent suppression of the $\bar{\nu}_e$ rate, and therefore negligibly affect $\langle E_{\bar{\nu}_e} \rangle$. Fig. 7A gives an example of this situation.

5 Conclusions

We have performed in [1] a systematical study of the effect of an extra sterile neutrino in all possible contexts, for any choice of its mixing parameters with the active neutrinos and fully including the active/active mixings now established by the results on solar and atmospheric oscillations. We considered cosmology (BBN, CMB, LSS), astrophysics (the Sun, SN...) and terrestrial neutrino experiments (atmospheric neutrinos, reactors, short- and long-base line beams). In these Proceedings I presented in detail the analysis relative to the effects in cosmology and in

supernovæ focussing on the principles of the computational techniques and on the understanding of the results.

We find no evidence for a sterile neutrino in the present data; figure 8 collects the **presents constraints**, in the six limiting cases of mixing with a mass eigenstate $\nu_{1,2,3}$ or a flavor eigenstate $\nu_{e,\mu,\tau}$. Every specific model of a sterile neutrino identifies a point or a region in one of these spaces or in a suitable combination of them, and should therefore be compared with the reported bounds. In particular, I showed in Sec.3.2 that the region of the LSND sterile neutrino is excluded by the cosmological constraints (unless they are relaxed by some non-standard modification to cosmology).

Finally, I discussed promising **future probes** of sterile effects. In the context of the cosmological observations, it looks important to improve the measurements of the primordial ^4He and Deuterium abundances, overcoming the systematic uncertainties. It looks also especially important to exploit the complementarity of the two probes, that are differently sensitive to sterile neutrinos in several regions of the parameter space, also in order to constrain the non-standard cosmological modifications. Moreover, future measurements of the CMB and LSS power spectra will expand the tested range of sterile parameters. Concerning supernovæ the best improvement would come from ... the occurring of a new explosion, which would allow to probe sterile effects through the predictions on the neutrino flux and spectrum, in regions that are not easily accessible to other tools (thanks to the long base-line and the extreme matter effects). Although progress must also come on the overall theoretical uncertainties of SN models, most of the results could be neat enough.

Other important probes for sterile neutrino effects are discussed in [1]: among them, solar neutrino experiments at sub-MeV energies and proposed reactor and LBL experiments look most interesting.

Acknowledgments

I thank Guido Marandella, Alessandro Strumia, Francesco Vissani, Yi-Zen Chu and the organizers of the IFAE 2004 and PASCOS'04 conferences. Work supported by the USA DoE grant DE-FG02-92ER-40704.

References

- [1] M. Cirelli, G. Marandella, A. Strumia, F. Vissani, “Probing oscillations into sterile neutrinos with cosmology, astrophysics and experiments”, hep-ph/0403158, Nucl.Phys. B in press.
- [2] **Solar neutrinos exclude a dominant sterile neutrino:** Q. R. Ahmad *et al.* [SNO Collaboration], Phys. Rev. Lett. **89** (2002) 011301 [arXiv:nucl-ex/0204008]. For additional discussion see e.g. P. Creminelli, G. Signorelli and A. Strumia, updated as arXiv:hep-ph/0102234v5 (also as JHEP **0105**, 052 (2001)); A. Bandyopadhyay *et al.*, Phys. Lett. B **583**, 134 (2004) [arXiv:hep-ph/0309174]; T. Schwetz, arXiv:hep-ph/0311217; B. C. Chauhan and J. Pulido, arXiv:hep-ph/0406227. For a complete discussion see Sec.4 of [1].
- [3] **Atmospheric neutrinos exclude a dominant sterile neutrino:** S. Fukuda *et al.* [Super-Kamiokande Collaboration], Phys. Rev. Lett. **85** (2000) 3999 [arXiv:hep-ex/0009001] and, more recently, see e.g. the talk by K. Okumura at the NO-VE workshop, Venice 3–5 dec. 2003, available at the web page axpd24.pd.infn.it/NO-VE/NO-VE.html. M. Ambrosio *et al.* [MACRO Collaboration], Phys. Lett. B **517**, 59 (2001) [arXiv:hep-ex/0106049]. For additional discussion see however R. Foot, Phys. Lett. B496 (2000) 169 (hep-ph/0007065) and R. Foot, hep-ph/0303005. For a complete discussion see Sec.6 of [1].
- [4] **Models with sterile neutrinos:** Light fermions from a discrete symmetry: E. Ma, P. Roy, Phys. Rev. D52 (1995) 4780. From a continuous symmetry: E. Ma, Mod. Phys. Lett. A11 (1996) 1893. From a supersymmetric R -symmetry: E.J. Chun, A.S. Joshipura, A.Yu. Smirnov, Phys. Lett. B357 (1995) 608. As Goldstone particles: E.J. Chun, A.S. Joshipura, A.Yu. Smirnov, Phys. Rev. D54 (1996) 4654. As modulinos: K. Benakli, A.Yu. Smirnov, Phys. Rev. Lett. 79 (1997) 4314. From a mirror world: S.I. Blinikov, M. Yu Khlopov, Sov. Astron. 27 (1983) 371. Z. Silagadze, Phys. Atom. Nucl. 60 (1997) 272 (hep-ph/9503481). R. Foot, R. Volkas, Phys. Rev. D52 (1995) 6595 (hep-ph/9505359). Z.G. Berezhiani, R.N. Mohapatra, Phys. Rev. D52 (1995) 6607 (hep-ph/9505385). V. Berezhinsky, M. Narayan, F. Vissani, hep-ph/0210204. From compositeness: N. Arkani-Hamed, Y. Grossman, hep-ph/9806223. From GUT representations: M. Bando, K. Yoshioka, Prog. Theor. Phys. 100 (1998) 1239 (hep-ph/9806400). From flat extra dimensions: K. R. Dienes, E. Dudas and T. Gherghetta, Nucl. Phys. B **557** (1999) 25 [arXiv:hep-ph/9811428]; N. Arkani-Hamed, S. Dimopoulos, G. R. Dvali and J. March-Russell, Phys. Rev. D **65** (2002) 024032 [arXiv:hep-ph/9811448]. G. R. Dvali and A. Y. Smirnov, Nucl. Phys. B **563** (1999) 63 [arXiv:hep-ph/9904211]. Models with 2 (or more) sterile neutrinos: W. Krolkowski, hep-ph/0402183; K. L. McDonald, B. H. J. McKellar and A. Mastrano, hep-ph/0401241; K. S. Babu and G. Seidl, hep-ph/0312285 and arXiv:hep-ph/0405197.

- [5] **Recent invocations of sterile neutrinos:** Sterile neutrinos to give pulsars a kicks: A. Kusenko, arXiv:astro-ph/9903167. To build up Dark Matter: X. d. Shi and G. M. Fuller, *Phys. Rev. Lett.* **82** (1999) 2832 [arXiv:astro-ph/98110076]. To account for the diffuse galactic ionization: R. N. Mohapatra and D. W. Sciama, arXiv:hep-ph/9811446. To make an effective r-process nucleosynthesis: G. C. McLaughlin, J. M. Fetter, A. B. Balantekin and G. M. Fuller, *Phys. Rev. C* **59** (1999) 2873 [arXiv:astro-ph/9902106]. To explain the low chlorine rate (now less necessary, see v4 of this same paper): P. C. de Holanda and A. Y. Smirnov, *Phys. Rev. D* **69**, 113002 (2004) [arXiv:hep-ph/0307266].
- [6] A. Aguilar *et al.* [LSND Collaboration], *Phys. Rev. D* **64** (2001) 112007 [arXiv:hep-ex/0104049].
- [7] **BBN:** For an old but still useful review see R.V. Wagoner, W.A. Fowler, F. Hoyle, *The Astrophys. J.* 148 (1967) 3. For a recent review see S. Sarkar, *Rept. Prog. Phys.* 59 (1996) 1493 (*hep-ph/9602260*). For precision computations, see D.A. Dicus *et al.*, *Phys. Rev. D* 26 (1982) 2694; R.E. Lopez, M.S. Turner, *Phys. Rev. D* 59 (1999) 103502 (*astro-ph/9807279*); S. Esposito *et al.*, *Nucl. Phys.* B568 (421) 2000 (*astro-ph/9906232*).
- [8] **WMAP:** C. L. Bennett *et al.*, *Astrophys. J. Suppl.* **148** (2003) 1 [arXiv:astro-ph/0302207]; D. N. Spergel *et al.*, *Astrophys. J. Suppl.* **148** (2003) 175 [arXiv:astro-ph/0302209].
- [9] G. Mangano, G. Miele, S. Pastor and M. Peloso, *Phys. Lett. B* **534** (2002) 8 [arXiv:astro-ph/0111408].
- [10] N_ν **from BBN:** P. Di Bari, *Phys. Rev. D* 65 (2002) 043509 (*hep-ph/0108182*) and addendum: P. Di Bari, *Phys. Rev. D* 67 (2003) 127301 (*hep-ph/0302433*); R. H. Cyburt, B. D. Fields, K. A. Olive, *Phys. Lett. B* 567 (2003) 227 (*astro-ph/0302431*); S. Hannestad as cited in [18]; V. Barger *et al.*, *hep-ph/0305075*; K.N. Abazajian, *Astropart. Phys.* 19 (2003) 303 (*astro-ph/0205238*); A. Cuoco *et al.*, *astro-ph/0307213*.
- [11] Start with L. Kawano, “Let’s go: Early universe. 2. Primordial nucleosynthesis: The Computer way,” FERMILAB-PUB-92-004-A; then track the successive implementations. The state-of-the-art is presented in P. D. Serpico *et al.*, *astro-ph/0408076*.
- [12] **Sterile/active oscillations and BBN** have been discussed in: D. Kirilova, Dubna preprint JINR E2-88-301. R. Barbieri, A. Dolgov, *Phys. Lett.* B237 (1990) 440. K. Enqvist *et al.*, *Phys. Lett.* B249 (1990) 531. K. Kainulainen, *Phys. Lett.* B244 (1990) 191. R. Barbieri, A. Dolgov, *Nucl. Phys.* B349 (1991) 743. K. Enqvist *et al.*, *Nucl. Phys.* B373 (1992) 498. J.M. Cline, *Phys. Rev. Lett.* 68 (1992) 3137. X. Shi, D.N. Schramm, B.D. Fields, *Phys. Rev. D* 48 (1993) 2563. E. Lisi, S. Sarkar, F.L. Villante, *Phys. Rev. D* 59 (1999) 123520 (*hep-ph/9901404*). A.D. Dolgov, F.L. Villante, *hep-ph/0308083*.
- [13] **Neutrino oscillations in the Early Universe.** A. Dolgov, *Sov. J. Nucl. Phys.* 33 (1981) 700. L. Stodolsky, *Phys. Rev. D* 36 (1987) 2273. A. Manohar, *Phys. Lett.* B186 (1987) 370. M.J. Thomson, B.H.J. McKellar, *Phys. Lett.* B259 (1991) 113. J. Pantaleone, *Phys. Lett.* B287 (1992) 128. A. Friedland, C. Lunardini, *hep-ph/0304055*. The formalism is clearly summarized in G. Sigl, G. Raffelt, *Nucl. Phys.* B406 (1993) 423. The dominant contribution to the refraction index was discussed in D. Nötzold, G. Raffelt, *Nucl. Phys.* B307 (1988) 924. A possible alternative approach could come from the formalism being introduced in V. A. Naumov, *Phys. Lett.* B529 (2002) 199 (*hep-ph/0112249*).
- [14] A.D. Dolgov, *Phys. Rept.* 370 (2002) 333 (*hep-ph/0202122*).
- [15] **Neutrino asymmetries in the Early Universe:** R. Foot, M.J. Thomson, R.R. Volkas, *Phys. Rev. D* 53 (1996) 5349. D.P. Kirilova, M.V. Chizhov, *Phys. Rev. D* 58 (1998) 073004 (*hep-ph/9707282*). D.P. Kirilova, M.V. Chizhov, *Nucl. Phys.* B591 (2000) 457 (*hep-ph/9909408*). A.D. Dolgov *et al.*, *Nucl. Phys.* B632 (2002) 363. V. Barger *et al.*, *Phys. Lett.* B569 (2003) 123 (*hep-ph/0306061*).
- [16] **Recent determinations of the ^4He primordial abundance:** B. E. J. Pagel, E. A. Simonson, R. J. Terlevich and M. G. Edmunds, *Mon. Not. Roy. Astron. Soc.* **255** (1992) 325. K. A. Olive and G. Steigman, *Astrophys. J. Suppl.* **97** (1995) 49 [arXiv:astro-ph/9405022]. Y. I. Izotov and T. X. Thuan, *Astrophys. J.* **500** (1998) 188. K. A. Olive, E. Skillman and G. Steigman, *Astrophys. J.* **483** (1997) 788 [arXiv:astro-ph/9611166]. Y. I. Izotov, F. H. Chaffee, C. B. Foltz, R. F. Green, N. G. Guseva and T. X. Thuan, *Astrophys. J.* **527** (1999) 757, arXiv:astro-ph/9907228. T. X. Thuan and Y. I. Izotov, in “The Light Elements and their Evolution”, Proceedings of IAU Symposium 198, held 22-26 Nov 1999, Natal, Brazil. Edited by L. da Silva, R. de Medeiros, & M. Spite, 2000., p.176, arXiv:astro-ph/0003234. M. Peimbert, A. Peimbert and M. T. Ruiz, *Astrophys. J.* **541** (2000) 688, arXiv:astro-ph/0003154. A. Peimbert, M. Peimbert and V. Luridiana, *Astrophys. J.* **565** (2002) 668-680, arXiv:astro-ph/0107189. S. Sarkar, “Neutrinos from the big bang,”

- Proc.Indian Natl.Sci.Acad.70A:163-178,2004, arXiv:hep-ph/0302175. Y. I. Izotov and T. X. Thuan, *Astrophys. J.* **602** (2004) 200 [arXiv:astro-ph/0310421]. K. A. Olive and E. D. Skillman, arXiv:astro-ph/0405588. The very interesting possibility of determining the ^4He abundance with a completely independent technique (namely from its birthmark on CMB alone) unfortunately looks promising only in the far future, if ever: R. Trotta and S. H. Hansen, *Phys. Rev. D* **69**, 023509 (2004) [arXiv:astro-ph/0306588]; and R. Trotta, arXiv:astro-ph/0410115; see also G. Huey, R. H. Cyburt and B. D. Wandelt, *Phys. Rev. D* **69**, 103503 (2004) [arXiv:astro-ph/0307080].
- [17] **Recent determinations of the D primordial abundance:** D. Kirkman, D. Tytler, S. Burles, D. Lubin, J.M. O’Meara, *Astrophys. J.* 529 (2000) 665. J. M. O’Meara, D. Tytler, D. Kirkman, N. Suzuki, J.X. Prochaska, D. Lubin, A.M. Wolfe, *Astrophys. J.* 552 (2001) 718. D. Kirkman, D. Tytler, N. Suzuki, J.M. O’Meara, D. Lubin, *astro-ph/0302006*. M. Pettini, D.V. Bowen, *Astrophys. J.* 560 (2001) 41. S. D’Odorico, M. Dessauges-Zavadsky, P. Molaro, *Astronomy and Astrophysics* 368 (2001)L21. S.A. Levshakov, P. Molaro, M. Dessauges-Zavadsky, S. D’Odorico, *Astrophys. J.* 565 (2002) 696.
- [18] The **cosmological bound on neutrino masses** is obtained by combining WMAP data with large-scale structure (and possibly other) data, see the papers in [8] and references therein. This is similar to pre-WMAP analyses, e.g. A. Lewis, S. Bridle, *Phys. Rev. D* 66 (2002) 103511.
- Other (sometimes more conservative) analysis find similar (sometimes weaker) bounds: S. Hannestad, *JCAP* 0305 (2003) 004 (*astro-ph/0303076*); S.W. Allen, R.W. Schmidt, S.L. Bridle, *Mon. Not. Roy. Astron. Soc.* 346 (2003) 593 (*astro-ph/0306386*); M. Tegmark et al. [SDSS Collaboration], *Phys. Rev. D* 69 (2004) 103501 (*astro-ph/0310723*); V. Barger et al., *Phys. Lett. B* 595 (2004) 55 (*hep-ph/0312065*), P. Crotty, J. Lesgourgues, S. Pastor, *Phys. Rev. D* 69 (2004) 123007 (*hep-ph/0402049*). More recent analysis: U. Seljak et al., *astro-ph/0407372*, G. L. Fogli et al., *hep-ph/0408045*. Crucial is the inclusion of the controversial $\text{Ly}\alpha$ data, as e.g. discussed in the latter. The robustness of the bound in presence of non-adiabatic incoherent fluctuations is studied in R.H. Brandenberger, A. Mazumdar, M. Yamaguchi, *Phys. Rev. D* 69 (2004) 081301 (*hep-ph/0401239*). Bounds on $\sum m_i$ from CMB data alone are not so stringent at present (see e.g. K. Ichikawa, M. Fukugita and M. Kawasaki, *astro-ph/0409768*) but could become so in the future (see e.g. M. Kaplinghat, L. Knox and Y. S. Song, *Phys. Rev. Lett.* 91 (2003) 241301 (*astro-ph/0303344*)).
- [19] D. J. Eisenstein, W. Hu and M. Tegmark, *Astrophys. J.* **518** (1998) 2 [arXiv:astro-ph/9807130]. J. Lesgourgues, S. Pastor and L. Perotto, *Phys. Rev. D* **70**, 045016 (2004) [arXiv:hep-ph/0403296].
- [20] For a useful review see S. Bashinsky, U. Seljak, *Phys. Rev. D* 69 (2004) 083002 (*astro-ph/0310198*).
- [21] N_ν **from CMB:** P. Crotty, J. Lesgourgues, S. Pastor, *astro-ph/0302337* *Phys. Rev.* 671230052003; E. Pierpaoli, *astro-ph/0302465* *Mon. Not. Roy. Astron. Soc.* 342L632003; V. Barger, J. P. Kneller, H. S. Lee, D. Marfatia, G. Steigman, *hep-ph/0305075* *Phys. Lett. B* 56682003; S. Hannestad as cited in [18].
- [22] A. Strumia, *Phys. Lett. B* **539** (2002) 91 [arXiv:hep-ph/0201134]; C. Giunti, *Mod. Phys. Lett. A* **18** (2003) 1179 [arXiv:hep-ph/0302173].
- [23] M. Maltoni, T. Schwetz, M. A. Tortola and J. W. F. Valle, *Nucl. Phys. B* **643**, 321 (2002) [arXiv:hep-ph/0207157].
- [24] **Non-standard cosmological (sterile) neutrino possibilities:** G. Gelmini, S. Palomares-Ruiz and S. Pascoli, *Phys. Rev. Lett.* **93**, 081302 (2004) [arXiv:astro-ph/0403323]; Z. Chacko, L. J. Hall, S. J. Oliver and M. Perelstein, arXiv:hep-ph/0405067; J. F. Beacom, N. F. Bell and S. Dodelson, *Phys. Rev. Lett.* **93**, 121302 (2004) [arXiv:astro-ph/0404585]; R. N. Mohapatra and S. Nasri, arXiv:hep-ph/0407194.
- [25] See e.g. some of the papers in [10] and references therein, plus A. Dolgov and F. Villante in [12] and M. Maltoni, T. Schwetz, M. A. Tortola and J. W. F. Valle, arXiv:hep-ph/0305312.
- [26] See the papers in [22], A. Pierce and H. Murayama, *Phys. Lett. B* **581** (2004) 218 [arXiv:hep-ph/0302131] and M. Maltoni et al. in [25].
- [27] **The SN1987a signal:** K. Hirata *et al.* [KAMIOKANDE-II Collaboration], *Phys. Rev. Lett.* **58** (1987) 1490; R. M. Bionta *et al.*, *Phys. Rev. Lett.* **58** (1987) 1494.
- [28] For a recent review see e.g. F. Cei, *Int. J. Mod. Phys. A* 17 (2002) 1765 (*hep-ex/0202043*).

- [29] **Sterile neutrinos and Supernovæ:** Neutrino oscillations in SN were discussed in S.P. Mikheev, A.Yu. Smirnov, *Sov. Phys. JETP* 64 (1986) 4. Bounds on sterile oscillations from the SN1987a rate were discussed in S.P. Mikheev, A.Yu. Smirnov, *JETP Lett.* 46 (1987) 10. X. Shi, G. Sigl, *Phys. Lett.* B323 (1994) 360 (*hep-ph/9312247*). H. Athar, J.T. Peltoniemi, *Phys. Rev. D* 51 (1995) 5785. H. Nunokawa, J. T. Peltoniemi, A. Rossi, J. W. F. Valle, *Phys. Rev. D* 56 (1997) 1704 (*hep-ph/9702372*). A. D. Dolgov, S. H. Hansen, G. Raffelt, D. V. Semikoz, *Nucl. Phys.* B590 (2000) 562 (*hep-ph/0008138*). P. Keranen, J. Maalampi, M. Myrskylainen, J. Riittinen, *hep-ph/0401082*. The physics of SNe in presence of sterile neutrinos from ExtraDimensions is also studied in G. Cacciapaglia et al., *Phys. Rev. D* 67, 053001 (2003) [arXiv:hep-ph/0209063] and *Phys. Rev. D* 68, 033013 (2003) [arXiv:hep-ph/0302246].
- [30] On this subject, see also the discussion in A. Friedland, *Phys. Rev. D* 64 (2001) 013008 [arXiv:hep-ph/0010231].
- [31] M. Th. Keil, G. G. Raffelt, H.-T. Janka, *Astrophys. J.* 590 (2003) 971 (*astro-ph/0208035*).
- [32] T.A. Thompson, A. Burrows, P.A. Pinto, *Astrophys. J.* 592 (2003) 434 (*astro-ph/0211194*)
- [33] F.J. Botella, C.S. Lim, W.J. Marciano, *Phys. Rev. D* 35 (1987) 896.
- [34] P. Vogel, J.F. Beacom, *Phys. Rev. D* 60 (1999) 053003 (*hep-ph/9903554*); A. Strumia, F. Vissani, *Phys. Lett.* B564 (2003) 42 (*astro-ph/0302055*).